

# Calculated Exchange Interactions and Competing S=0 and S=1 States in Doped NdNiO<sub>2</sub>

Xiangang Wan\*, Vsevolod Ivanov<sup>†</sup>, Giacomo Resta<sup>†</sup>, Ivan Leonov<sup>††</sup>, Sergey Y. Savrasov<sup>†</sup>

<sup>\*</sup>National Laboratory of Solid State Microstructures,

School of Physics and Collaborative Innovation Center of Advanced Microstructures, Nanjing University, 210093 Nanjing

<sup>†</sup>Department of Physics and Astronomy, University of California, Davis, CA 95616 and

<sup>††</sup>M.N. Miheev Institute of Metal Physics, Russian Academy of Sciences and Ural Federal University, 620002 Yekaterinburg

(Dated: September 14, 2022)

Using density functional based LDA+U method and linear-response theory, we study the magnetic exchange interactions of the superconductor Nd<sub>1-x</sub>Sr<sub>x</sub>NiO<sub>2</sub>. We find that the hole doping increases the magnetic moment of the Ni-3d<sub>3z<sup>2</sup>-r<sup>2</sup></sub> orbital and significantly enhances the inter-layer exchange coupling. This can be understood in terms of small hybridization of Ni-3d<sub>3z<sup>2</sup>-r<sup>2</sup></sub> within the NiO<sub>2</sub> plane which results in a flat band near the Fermi level, and its large overlap along z direction. We also demonstrate that the Nd-5d states appearing at the Fermi level, do not affect the magnetic exchange interactions, and thus may not participate in the superconductivity of this compound. Whereas many previous works emphasize the importance of the Ni-3d<sub>x<sup>2</sup>-y<sup>2</sup></sub> and Nd-5d orbitals, we instead propose that the material can be described by a Ni-3d<sub>x<sup>2</sup>-y<sup>2</sup></sub>/Ni-3d<sub>3z<sup>2</sup>-r<sup>2</sup></sub> two-band model. Its solution is studied here on the level of Dynamical Mean Field Theory and reveals an underlying Mott insulating state which, depending on precise values of the intra-atomic Hund's coupling, produces upon doping competing S=0 and S=1 two-hole states at low energies that lead to very different quasiparticle band structures. We propose that trends upon doping in spin excitation spectrum and quasiparticle density of state can be a way to probe Ni 3d<sup>8</sup> configuration.

PACS numbers:

## I. INTRODUCTION

Since the discovery of high-temperature superconductors (HTSCs)[1], tremendous theoretical and experimental efforts have been devoted to understanding the novel physics of this family of compounds[2–4]. All HTSCs are comprised of quasi-two-dimensional CuO<sub>2</sub> planes separated by charge reservoir spacer layers, and their parent compounds have antiferromagnetic (AFM) order with very strong in-plane magnetic exchange interactions, belonging to the class of charge-transfer insulators[5]. Upon doping, holes occupy the O-2p orbital, and due to the strong hybridization between Cu-3d<sub>x<sup>2</sup>-y<sup>2</sup></sub> and O-2p orbitals, a Zhang-Rice singlet is formed[6]. It has been widely accepted that the HTSCs can be described by an effective single band t-J model, with different parameters explaining the variation in T<sub>c</sub> in different materials [7, 8].

Inspired by HTSCs, the search for possible novel superconducting behavior in nickelates has been attracting significant attention, as their structure and electronic configuration is similar to that of the cuprates [9–12]. Unfortunately, the monovalent Ni ion is strongly unstable and scarcely formed in mineral compounds, making, for example, LaNiO<sub>2</sub> difficult but possible to synthesize[10]. First-principles Local Density Approximation (LDA) based calculations revealed an important difference between LaNiO<sub>2</sub> and its sister infinite-layer HTSC compound CaCuO<sub>2</sub>: the Fermi surface of CaCuO<sub>2</sub> consists of only one two-dimensional band, while LaNiO<sub>2</sub> seems quite three-dimensional, with La-derived 5d states and

Ni-3d states crossing the Fermi level[13]. Numerical calculations predicted AFM magnetic order[13, 14], but magnetization and neutron powder diffraction observe no long-range order in LaNiO<sub>2</sub>[11]. At high temperatures (150K < T < 300K), the susceptibility of LaNiO<sub>2</sub> can be fitted by the sum of a temperature independent term, and a Curie-Weiss S = 1/2 paramagnetic term with a large Weiss constant (θ = -257K), indicating a significant correlation between Ni spins[11]. LaNiO<sub>2</sub> shows metallic behavior, but resistivity increases at lower temperatures and no superconducting state has been observed [9–11].

Recently, Nd<sub>0.8</sub>Sr<sub>0.2</sub>NiO<sub>2</sub> thin films were synthesized on a SrTiO<sub>3</sub> substrate using soft-chemistry topotactic reduction, and superconductivity with considerably high T<sub>c</sub> (up to 15K) was observed[15]. The superconducting phase displays a doping-dependent dome for Nd<sub>1-x</sub>Sr<sub>x</sub>NiO<sub>2</sub> (0.125 < x < 0.25), which is remarkably similar to that of the cuprates [16, 17]. Very recently, superconductivity has also been observed in doped PrNiO<sub>2</sub>[18].

These breakthroughs have stimulated large-scale theoretical efforts to understand the nature of the superconductivity in rare-earth nickelates[19]–[52]. LDA band structures predict that both Nd-5d and Ni-3d<sub>x<sup>2</sup>-y<sup>2</sup></sub> orbitals contribute significantly to the Fermi surface of parent compound NdNiO<sub>2</sub>. Most calculations treat the three 4f electrons in Nd<sup>3+</sup> as core electrons, although the role of Nd-4f has been emphasized recently[20]. Many-body perturbative GW calculations result in almost no modification to the Fermi-surface topology and its orbital composition[21]. Focusing on the Fermi surface, differ-

ent minimal models have been proposed to describe the low energy physics of this material using a Wannier function approach, including: a three-band model with Ni- $3d_{x^2-y^2}$ , Nd- $5d_{3z^2-r^2}$  and an interstitial  $s$  orbital[22]; a three-band model with Ni- $3d_{x^2-y^2}$ , Nd- $5d_{3z^2-r^2}$  and Nd- $5d_{xy}$ [23, 24]; a two-band model with Ni- $3d_{x^2-y^2}$  and Nd- $5d_{3z^2-r^2}$ [26, 30]; and a four-band model[27]. The effect of topotactic hydrogen has been discussed as well[35].

Several works addressed strong correlation effects among Ni 3d electrons. Due to a large energy difference between O- $2p$  and Ni- $3d$  levels, the undoped NdNiO<sub>2</sub> has been suggested to be a Mott insulator, and a coexistence/competition between low energy S=0 and S=1 states has been proposed for the hole doped case [19] where some Ni ions would acquire a formal  $3d^8$  configuration. The origin of these two-hole states has been discussed in a recent literature[25, 43, 47, 49, 51]. As it is commonly accepted that the undoped Ni  $3d^9$  configuration corresponds to the hole of  $x^2 - y^2$  symmetry, the two-hole states produced by doping can either end up as intraorbital singlets or interorbital triplets. It has been first pointed out[19] that the S=1 state maybe incompatible with robust superconductivity, and indeed exact diagonalization study of Ni impurity embedded into the oxygen environment [19] as well as a number of many-body calculations using a combination of LDA with Dynamical Mean Field Theory (DMFT)[25, 43] pointed to the formation of the intraorbital singlets. On the other hand, a variant of the t-J model with S=1 has been proposed and shown to exhibit d-wave superconductivity[49]. Symmetries of the pairing states based on a two-orbital Ni- $3d_{x^2-y^2}$ /Ni- $3d_{xy}$  model Hamiltonian with competing S=0 and S=1 two-hole states have been discussed[47]. DMFT calculations for the two-orbital Ni- $3d_{x^2-y^2}$ /Ni- $3d_{3z^2-r^2}$  system argued that a multiorbital description of nickelate superconductors is necessary [51]. Excitations and superconducting instabilities have also been explored by a random phase approximation [29] and by a variant of the t-J model[40]. Local spin, charge and orbital susceptibilities have been calculated using a combination of DMFT with a local quasiparticle self-consistent GW method and emphasized the Hund's physics of Ni- $e_g$  electrons[41].

No sign of magnetic order has been observed in NdNiO<sub>2</sub>[15], which may be attributed to defects, such as unwanted hydrides or hydroxides that might form as by-products of the creation of the rare Ni<sup>+</sup> oxidation state during the synthesis of this compound. Another consideration is that LaNiO<sub>3</sub> is close to an antiferromagnetic quantum critical point (QCP)[36], therefore it is reasonable to expect that with lower dimensionality, NdNiO<sub>2</sub> would pass the QCP and display magnetism. Very recently, strong spin fluctuations and considerable AFM exchange interactions have been observed in NdNiO<sub>2</sub>[37]. The exchange interactions have also been discussed in several works [23][31][32][33]. The calculated electron-

phonon interaction ( $\lambda \leq 0.32$ ) is too small to explain the 15K T<sub>c</sub> in this material[22], meaning the spin excitations, which are thought to be responsible for the superconductivity in HTSCs[2][3][4], are worth careful investigation.

In this work, based on a density functional LDA+U method and linear-response theory[53], we perform detailed studies of exchange interactions for both parent and doped NdNiO<sub>2</sub>. The method does not rely on a total energy analysis, and instead directly computes the exchange constant for a given wave vector  $\mathbf{q}$  based on the result of the magnetic force theorem [54]. Our results show that although the Fermi surface of undoped NdNiO<sub>2</sub> is quite three-dimensional, its magnetic exchange interaction  $J$  has a clear two-dimensional feature with considerable in-plane  $J_1$  and negligible out-of-plane  $J_{z1}$ . However, the Ni- $3d_{3z^2-r^2}$  band close to the Fermi level is quite flat, therefore within the LDA+U method for a reasonable range of the values of Hubbard  $U$  above 4 eV, holes introduced by doping preferentially occupy the Ni- $3d_{3z^2-r^2}$  orbitals while Ni- $t_{2g}$  states remain remarkably inert. The in-plane  $J_1$  remains almost unchanged with doping, but the magnetic moment of the Ni- $3d_{3z^2-r^2}$  orbital and the out-of-plane  $J_{z1}$  both grow significantly. Our calculation using a constrained-orbital-hybridization method [55] unambiguously demonstrates that while Nd- $5d$  makes an important contribution to the Fermi surface, it has almost no effect on the magnetic exchange interaction. This means the magnetic excitations in hole-doped NdNiO<sub>2</sub> can be described by an effective Ni- $3d_{x^2-y^2}$ /Ni- $3d_{3z^2-r^2}$  two-band model.

To gain additional insight, we discuss the solutions of such two-band model on the basis of Dynamical Mean Field Theory using the parameters deduced from our band structure calculations. In contrast to the static mean field description, such as LDA+U, where holes occupying Ni- $3d_{3z^2-r^2}$  states promote interorbital triplets, competing S=0 and S=1 states emerge from our DMFT simulation which, depending on a precise value of the intraatomic Hund's rule exchange, lead to very different quasiparticle band structures. We thus propose that trends upon doping in magnetic exchange interactions and quasiparticle density of states can be a way to probe Ni  $3d^8$  configuration.

Our paper is organized as follows. In Section II we describe our LDA+U and constrained-orbital-hybridization calculations for the exchange interactions. In Section III, we discuss a minimal two-band model that emerges from our study and its solution based on Dynamical Mean Field Theory. Section IV is the conclusion.

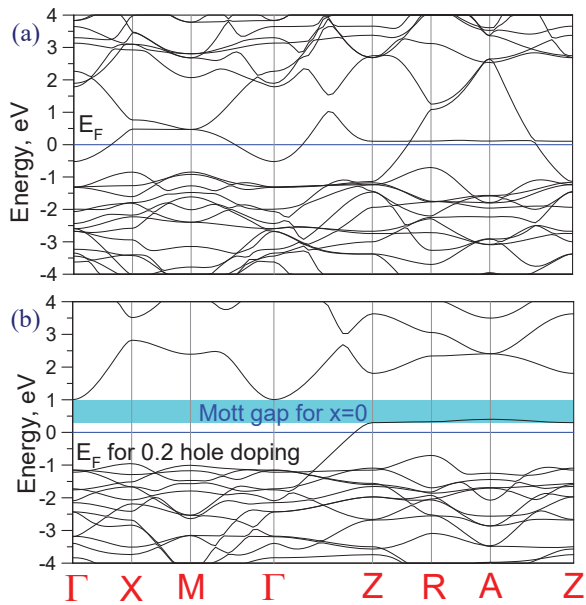


FIG. 1: Band structure of  $(\pi, \pi, 0)$  spin ordering from LDA+ $U$  calculations with  $U = 6.0\text{eV}$ .  $\Gamma$  (0, 0, 0), X (1/2, 0, 0), M (1/2, 1/2, 0), Z (0, 0, 1/2), R (1/2, 0, 1/2), A (1/2, 1/2, 1/2). (a) undoped NdNiO<sub>2</sub>, (b) constrained orbital-hybridization calculation for NdNiO<sub>2</sub> with the Nd-5d band shifted up by 2 Ry. The position of the Fermi level corresponds to 0.2 hole doping.

## II. CALCULATIONS OF EXCHANGE INTERACTIONS

We perform our density functional based electronic structure calculations within the full potential linear-muffin-tin-orbital (LMTO) method[56]. To take into account the effect of on-site electron-electron interactions between Ni-3d orbitals we add a correction due to Hubbard  $U$  using the so-called LDA+ $U$  approach[57]. We vary the parameter  $U$  for Ni-3d between 4.0 and 8.0 eV, and find that the essential properties and our conclusions do not depend on the value of  $U$  in this range. Below we report our results for exchange constants with  $U = 6$  eV and Hund's  $J_H = 0.95$  eV. Experimental lattice parameters have been used[15].

The magnetic exchange interactions  $J(\mathbf{q})$  were evaluated assuming a rigid rotation of atomic spins, using a previously developed linear-response approach [53]. This technique has been applied successfully to evaluate magnetic interactions for a series of materials, includ-

TABLE I: Calculated exchange interactions,  $J_1$  (in-plane nearest) and  $J_{z1}/J_{z2}$  (out-of-plane nearest/next-nearest) in meV for various hole dopings. Positive/negative sign denotes AFM/FM interaction. We also list the calculated total magnetic moment at the Ni site,  $M_{tot}$ , and magnetic moment at the Ni-3 $d_{3z^2-r^2}$  orbital,  $M_{3z^2-r^2}$ , (in  $\mu_B$ ).  $n_h$  denotes the doping (number of holes per unit cell).

| $n_h$ | $J_1$ | $J_{z1}$ | $J_{z2}$ | $M_{tot}$ | $M_{3z^2-r^2}$ |
|-------|-------|----------|----------|-----------|----------------|
| 0.05  | 17.96 | -5.35    | -5.60    | 1.03      | 0.23           |
| 0.10  | 16.50 | -9.85    | -4.62    | 1.07      | 0.27           |
| 0.15  | 16.14 | -14.75   | -2.76    | 1.08      | 0.29           |
| 0.20  | 14.65 | -20.19   | -1.25    | 1.14      | 0.35           |
| 0.25  | 14.14 | -24.35   | -1.21    | 1.16      | 0.37           |
| 0.30  | 12.87 | -26.76   | -0.72    | 1.22      | 0.43           |

ing transition-metal oxides[53], HTSCs[58], Fe-based superconductors[59]; europium monochalcogenides[60], orbital-ordered noncollinear spinel MnV<sub>2</sub>O<sub>4</sub>[61], and Dirac magnon material Cu<sub>3</sub>TeO<sub>6</sub>[62]. We also use a constrained-orbital-hybridization method to provide theoretical insights into the various contributions[55] to the magnetic exchange interactions in hole doped NdNiO<sub>2</sub>. To avoid the effect of the very narrow Nd-4f bands, we shift the three occupied Nd-4f orbitals downward while shifting the rest of the Nd-4f band upward by using a constrained-orbital approach [55]. Since the obtained results do not depend on the magnitude of the shifts, we display the results with the Nd-4f bands shifted by  $\pm 2.0$  Ry.

Similarly to previously reported band structure calculations for LaNiO<sub>2</sub>[13, 22, 24, 27], there are two bands crossing the Fermi level in the LDA band structure of NdNiO<sub>2</sub>, with one band primarily derived from the Ni-3 $d_{x^2-y^2}$  orbital and the other consisting of predominantly Nd-5d character. Just as with LaNiO<sub>2</sub>[13, 22], there is a gap between Ni-3d and O-2p bands (around 3.5 eV). Moreover, Ni-O bond length in NdNiO<sub>2</sub> (1.96 Å) is slightly larger than the Cu-O bond length in CaCuO<sub>2</sub> (1.92 Å). Thus the bandwidth of the Ni-3 $d_{x^2-y^2}$  band correspondingly smaller than that of the Cu-3 $d_{x^2-y^2}$  band. While in both NdNiO<sub>2</sub> and CaCuO<sub>2</sub>, the 3 $d_{3z^2-r^2}$  orbitals have very small dispersions along the ZRAZ line, the dispersion of the Ni-3 $d_{3z^2-r^2}$  state along  $\Gamma Z$  is considerably larger than that of Cu-3 $d_{3z^2-r^2}$ . Moreover, compared to Cu-3 $d_{3z^2-r^2}$ , the Ni-3 $d_{3z^2-r^2}$  band lies closer to the Fermi level. These two features are expected to significantly affect the magnetic behavior in the hole doped NdNiO<sub>2</sub>.

We now perform the LDA+ $U$  calculation to examine magnetic exchange interactions in undoped NdNiO<sub>2</sub>. Our results show that the exchange coupling is short ranged and only important for the nearest-neighbor  $J_1$  within the NiO<sub>2</sub> plane. The sign of this term is AFM, and thus the NiO<sub>2</sub> layer shows a  $(\pi, \pi)$  spin ordering. There is some debate about the magnitude of the exchange in-

TABLE II: Calculated exchange interactions (in meV) for  $x=0.2$  hole doped NdNiO<sub>2</sub>, with Nd-5d shifted upward by various energies (in Ry).

| Shift (Ry): | $J_1$ | $J_{z1}$ |
|-------------|-------|----------|
| 0.05        | 16.07 | -21.01   |
| 0.10        | 16.37 | -20.94   |
| 0.50        | 17.42 | -18.88   |
| 2.00        | 17.98 | -19.74   |

teraction, with estimates ranging from much less than that of cuprates [19, 23, 31] to comparable to the value of exchange interaction in CaCuO<sub>2</sub>[30, 32, 33]. Our numerical  $J_1$  (20.56 meV) is about 18 % less than the value estimated from the two-magnon peak in the Raman scattering experiment[31, 37]. The in-plane  $J_1$  we compute is about five times less than that in CaCuO<sub>2</sub>[58]. This can be attributed to the smaller Ni-3d and O-2p hybridization and larger energy splitting between Ni-3d and O-2p as has previously been pointed out[13]. Consistent with the result of  $(\pi, \pi, 0)$  spin ordering being slightly more energetically favorable than  $(\pi, \pi, \pi)$ , our calculation produces a rather small out-of-plane FM exchange interaction, with nearest neighbor  $J_{1z} = -0.85$  meV and second nearest neighbor  $J_{2z} = -5.75$  meV, respectively. Our calculations reveal that the magnetic moment at the Ni site ( $1.04 \mu_B$ ), residing mostly in the  $3d_{x^2-y^2}$  orbital, is much larger than that at Cu sites in HSTCs.

There exists a fairly flat band right at the Fermi level along the  $ZRZ$  line, in the band structure of the magnetic ground state configuration of NdNiO<sub>2</sub>, as shown in Fig.1(a). This flat band has predominantly Ni- $3d_{3z^2-r^2}$  character, and plays an important role when hole doping is considered. The very small in-plane dispersion of the Ni- $3d_{3z^2-r^2}$  band can be understood as a consequence of the symmetry of the Ni- $3d_{3z^2-r^2}$  orbital, which can only weakly hybridize with the neighboring O-2p.

To examine the doping dependence we perform a series of hole-doped calculations, varying the number of holes per unit cell from 0.05 to 0.30 by using the virtual crystal approximation. These calculations show that the hole doping within this range does not significantly change the shape of the band structure apart from shifting the Fermi level downward. Regardless of the hole-doping concentration, the Ni- $t_{2g}$  band is almost fully occupied and does not contribute to the magnetic moment. The magnetic moment of the Ni- $3d_{x^2-y^2}$  orbital is also unaffected by the hole doping. Instead, the holes preferentially occupy the flat Ni- $3d_{3z^2-r^2}$  band, and, as a result, the magnetic moment of this orbital increases with doping as shown in Table I. Noting the considerable Ni- $3d_{3z^2-r^2}$  band dispersion along  $\Gamma Z$ , and the formation of magnetic moments in this orbital, one can expect the emergence of out-of-plane magnetic exchange interactions. This result has been confirmed by our linear response calculation. As shown in Table I, hole doping

significantly enhances the out-of-plane  $J_{z1}$ , while the in-plane  $J_1$  remains mostly unaffected.

The 5d orbital is spatially very wide, and can have a crucial effect on the magnetic exchange interaction through 4f-5d hybridization, even though it is empty and located above the Fermi level[60]. In NdNiO<sub>2</sub>, the Nd-5d band appears at the Fermi level, making it important to understand the role of the Nd-5d orbital in magnetic exchange interactions. We address this issue by using a constrained-orbital-hybridization approach[55]. We perform the calculations with the Nd-5d band shifted upward by various values. Fig. 1(b) shows the band structure for the case where the Nd-5d band is shifted upward by 2 Ry. As one can see, the AFM insulating state emerges from this calculation for the undoped case, while hole doping vacates the Ni- $3d_{3z^2-r^2}$  band within  $k_z = \pi/c$  plane.

Our calculation shows that both in-plane  $J_1$  and out-of-plane  $J_{z1}$  exchange interactions are not sensitive to the position of the Nd-5d band as shown in Table II, clearly indicating that the effect of this orbital on the magnetic exchange interactions is negligible. A similar calculation was performed for LaNiO<sub>2</sub> to further confirm these findings. While the obtained values of the exchange interactions are slightly different, the key features discussed above are the same.

We illustrate the effect of increasing out-of-plane exchange interactions in doped NdNiO<sub>2</sub>, using an antiferromagnetic Heisenberg model and plot its spin-wave dispersions for both undoped and 0.2 hole-doped NdNiO<sub>2</sub> in Fig. 2, along with those of CaCuO<sub>2</sub> for comparison[58]. Our model demonstrates the dramatic differences between the spin-wave dispersions of NdNiO<sub>2</sub> and CaCuO<sub>2</sub>. Notably, the peak around  $(\frac{1}{2}, 0, 0)$  is reduced in NdNiO<sub>2</sub> compared with CaCuO<sub>2</sub>, as a consequence of the smaller in-plane exchange couplings, and is largely unaffected by doping. In contrast, the out-of-plane exchange interactions strongly depend on doping, which can be seen in the changing dispersion along  $\Gamma Z$ . Thus, one can expect that in contrast with HTSCs, a strongly doping dependent resonance will be observed in neutron experiments. In undoped NdNiO<sub>2</sub>, a modest out-of-plane  $J_{z2} = -5.75$  meV dominates over the vanishing nearest neighbor  $J_{z1} = -0.85$  meV. Doping amplifies  $J_{z1}$  while suppressing  $J_{z2}$ , resulting in the disappearance of the valley at  $(0, 0, 1/2)$  in the dispersion.

### III. TWO-BAND MODEL

A minimal model for the electronic structure of NdNiO<sub>2</sub> that emerges from the present study should involve Ni- $3d_{x^2-y^2}$  and Ni- $3d_{3z^2-r^2}$  orbitals only. Its parameters can be obtained by tracing the orbital character of these states from the paramagnetic LDA calculation. We show this in red for Ni- $3d_{x^2-y^2}$  and in green

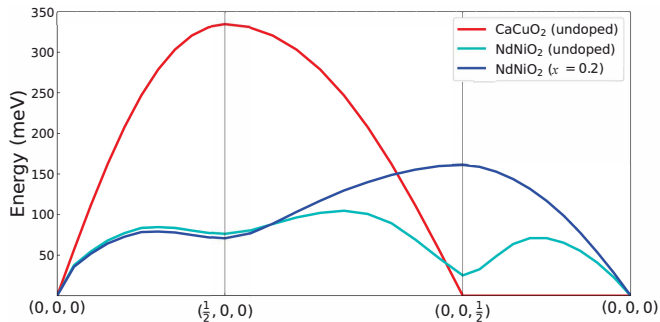


FIG. 2: Calculated spin-wave dispersions for the undoped NdNiO<sub>2</sub> (cyan), and 0.2 hole-doped NdNiO<sub>2</sub> (blue), with  $U=6\text{eV}$ . For comparison, we also plot the results of CaCuO<sub>2</sub> (red) [58].

for Ni- $3d_{3z^2-r^2}$  in Fig. 3(a). The derived two-band tight-binding model is illustrated in Fig. 3(b). In the large  $U$  limit, such model at a quarter filling by holes (3 electron filling) is expected to exhibit a Mott insulator for  $3d_{x^2-y^2}$  band, with the lower Hubbard band placed below  $3d_{3z^2-r^2}$  state. Its antiferromagnetic solution in the Hartree-Fock approximation will result in the band structure very similar to the LDA+ $U$  result shown in Fig. 1(b), which also assumes that the  $t_{2g}$  states of Ni, although appear in the same energy range, are apparently irrelevant. According to our LDA+ $U$  calculation with  $U \gtrsim 4$  eV, doping sends the holes primarily to the  $3d_{3z^2-r^2}$  state promoting interorbital triplets. This is seen in Fig. 1(b) where the Fermi level shifting downwards unoccupies the  $3d_{3z^2-r^2}$  band in  $k_z = \pi/c$  plane which explains doping dependence of the orbital occupancies shown in Table I.

The described picture should however be contrasted to the genuine strong correlation effect that prompts to consider an additional hole to be injected into either Ni  $x^2 - y^2$  or  $3z^2 - r^2$  orbital resulting either in an intra-orbital singlet or interorbital triplet. Therefore, in reality, it is not the relation of Hubbard  $U$  to the crystal field splitting  $\Delta$  between  $x^2 - y^2$  and  $3z^2 - r^2$  levels but the competition of the Hund's rule  $J_H$  and  $\Delta$  which should be examined to understand the origin of the two-hole state in the doped case [19, 25, 43, 51]. To illustrate the proximity of both ( $S=0$  and  $S=1$ ) solutions, a simple diagonalization of the  $3d^8$  shell with  $U=6$  eV and our deduced from Fig. 1(b) crystal field splitting  $\Delta=2.2$  eV reveals that the lowest energy state is  $S=0$  for  $J_H < 0.9$  eV, and  $S=1$  otherwise. This value is well within the range of generally assumed Hund's rule exchange energies for transition metal oxides and highlights a delicate balance in extracting the two-hole ground state configuration.

Although a number of full-fledge multiorbital LDA+DMFT calculations have been recently carried out to understand the many-body physics of doped NdNiO<sub>2</sub> [25, 43, 46], a strong sensitivity of the solution

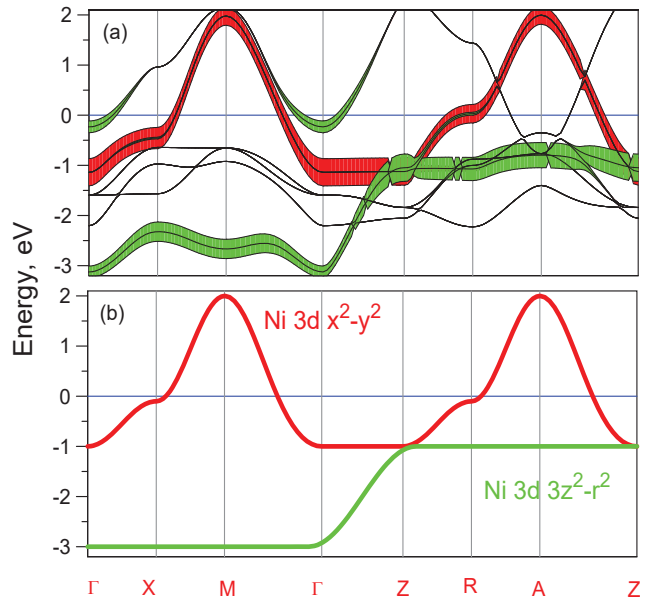


FIG. 3: (a) Paramagnetic LDA band structure of NdNiO<sub>2</sub> with the orbital character of Ni- $3d_{x^2-y^2}$  and Ni- $3d_{3z^2-r^2}$  states shown in red and green, respectively. (b) The corresponding two-band tight-binding model.

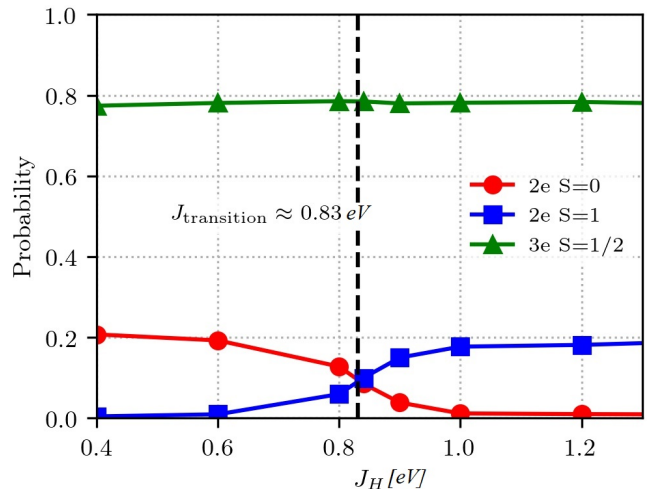


FIG. 4: Calculated probabilities for the three electron  $S=1/2$  and two-electron  $S=0$  and  $S=1$  states as a function of Hund's coupling  $J_H$  using Dynamical Mean Field Theory and Continuous Time Quantum Monte Carlo Method for the two-band model of NdNiO<sub>2</sub> corresponding to doping by 0.2 holes (filling by 2.8 electrons in the model). An inverse temperature of  $\beta = 40$  is used in the calculations.

to the input parameters, such as  $J_H$ , is expected. To gain further insight, here we study our derived two-band model using Dynamical Mean Field Theory [63] and Continuous Time Quantum Monte Carlo method [64]. The parameters  $U=6$  eV and  $\Delta=2.2$  eV are fixed while  $J_H$  is adjusted. The undoped case of Ni  $3d^9$   $S=1/2$  state corresponds to the electronic filling equal to 3 in this model,

where we easily recover a paramagnetic Mott insulating state with the gap of the order of  $U$  that opens up in the  $x^2 - y^2$  band and with the  $3z^2 - r^2$  states that remain completely occupied. Doping this model with 0.2 holes (filling by 2.8 electrons) results in finite probability to find either  $S=0$  or  $S=1$  states in addition to  $S=1/2$  that depends on  $J_H$ . These probabilities extracted from the Quantum Monte Carlo simulation are shown in Fig. 4. We can see that the transition between the low/high spin states occurs at  $J_H \approx 0.83$  eV which is very close to our earlier estimate of 0.9 eV.

Our results for the  $\mathbf{k}$ -resolved spectral functions are summarized in Fig. 5, where a comparative study is presented for the two quasiparticle band structures corresponding to  $S=0$  state ( $J_H$  is set to 0.6 eV, Fig. 5(a)) and to  $S=1$  state ( $J_H$  is set to 1 eV, Fig. 5(b)). One can see from the calculated spectrum for  $J_H = 0.6$  eV that the  $3z^2 - r^2$  state remains completely occupied while the doping primarily affects the  $x^2 - y^2$  band which now shows a typical for DMFT three-peak structure with the two Hubbard bands appearing below and above the Fermi level and a renormalized quasiparticle band that crosses  $E_F$ . The  $\mathbf{k}$  dispersion for all three features is similar to the original dispersion of the  $x^2 - y^2$  band.

A different picture emerges from the calculation with  $J_H = 1$  eV shown in Fig. 5(b). In this case, renormalized quasiparticles of the  $3z^2 - r^2$  character appear at the Fermi level which illustrate the formation of the interorbital triplet states. A very strong peak in the quasiparticle density of state is expected to be present at  $E_F$  due to the non-dispersive portion of the  $3z^2 - r^2$  band within the  $ZRA$  plane. At the same time, the  $x^2 - y^2$  band does not develop a three-peak structure and is characterized by the two Hubbard bands as in the undoped case.

Since the Hunds coupling  $J_H$  of 0.8 to 0.9 eV is well within the range of commonly accepted values, we cannot make a definite conclusion about whether  $S=0$  or  $S=1$  scenario is realized for doped nickelates. However, possible future angle-resolved photoemission (ARPES) experiments may provide important insight since as illustrated by our calculations the quasiparticle band structure is very different between the two cases. Furthermore, while ARPES spectra in the hole-doped HTSCs show waterfall-like behavior[65], we do not expect waterfalls to appear here due to a lack of oxygen states at energies close to  $E_F$  and associated physics responsible for the formation of the low energy states[66].

#### IV. CONCLUSION

In conclusion, using the LDA+U method, we have calculated magnetic exchange interactions for the doped NdNiO<sub>2</sub> novel superconductor. We find that the parent compound is mostly two-dimensional, with substantial in-plane, and minimal out-of-plane exchange inter-

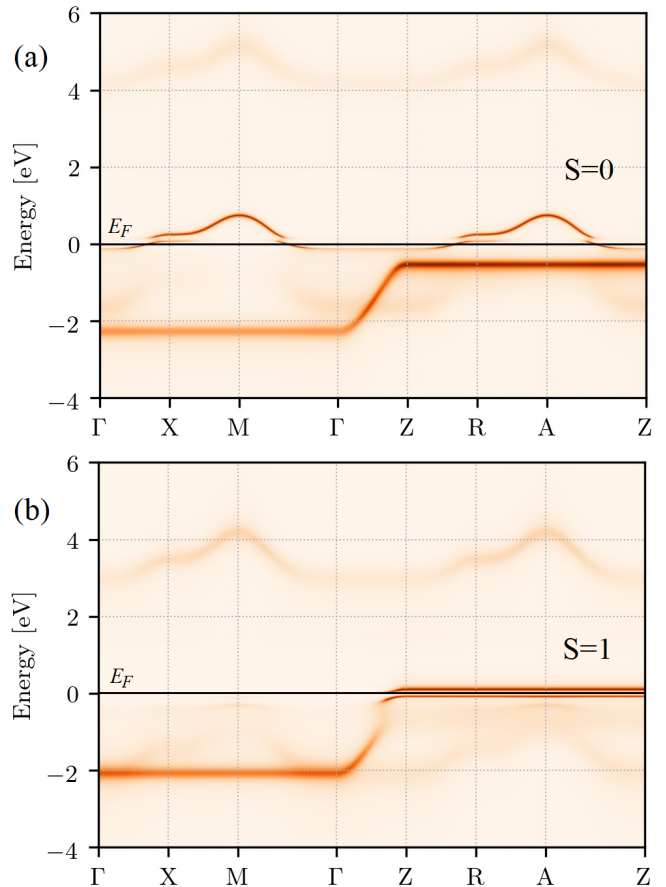


FIG. 5: Quasiparticle band structures of the two-band model of NdNiO<sub>2</sub> obtained by Dynamical Mean Field Theory and Continuum Time Quantum Monte Carlo Method for the doping level of 0.2 holes: (a) Calculation for Hunds coupling  $J_H = 0.6$  eV that corresponds to  $S=0$  two-hole state; (b) Calculation for  $J_H = 1$  eV corresponding to  $S=1$  two-hole state. An inverse temperature  $\beta = 40$  is used for the calculations.

actions. Upon doping, where the out-of-plane coupling  $J_{z1}$  increases dramatically, while the in-plane  $J_1$  is almost unchanged. To clarify the origin of these trends, we analyzed the symmetry of the holes induced by doping which were found to be primarily of the  $3d_{3z^2-r^2}$  character promoting the formation of interorbital triplet as Ni  $3d^8$  ground state configuration. We also investigated the role of the Nd- $5d$  states, which contribute substantially to the Fermi surface of NdNiO<sub>2</sub>. Shifting this band upward using a constrained-orbital-hybridization method has little effect on exchange interactions, which leads us to conclude that Nd- $5d$  states have negligible effect on the spin fluctuations and the superconductivity in NdNiO<sub>2</sub>. A minimal two-band model with active Ni- $3d_{x^2-y^2}$  and Ni- $3d_{3z^2-r^2}$  orbitals emerged from the present study. Its DMFT solution reveals an underly-

ing Mott insulating state which upon doping leads to a delicate competition between  $S=0$  and  $S=1$  two-hole states for the values of Hund's rule coupling in the range of 0.8 to 0.9 eV. Should  $S=1$  state be valid, we predict that upon doping the spin susceptibility gains three dimensionality as it gets enhanced along  $\Gamma Z$ . This can be readily observed in neutron experiments and can be one way to probe the two-hole configuration. We also predict a formation of a strong quasiparticle peak at the Fermi level detectable by ARPES experiments. A small anisotropy in  $H_{c2}$  was indeed discovered very recently [67] illustrating the three-dimensional nature of  $\text{NdNiO}_2$  which starkly contrasts with the two-dimensional superconductivity in HTSCs, and should be an important consideration in future studies of nickelate superconductors.

### ACKNOWLEDGEMENTS

X.W. is supported by the NSFC (Grants No. 11834006, No. 11525417, No. 51721001, and No. 11790311), National Key R&D Program of China (Grants No. 2018YFA0305704 and No. 2017YFA0303203). X.W. also acknowledges the support from the Tencent Foundation through the XPLOER PRIZE. V.I, G.R. and S.Y.S are supported by NSF DMR Grant No. 1832728. I.L. acknowledges support by the Russian Foundation for Basic Research (Project No. 18-32-20076). The DMFT electronic structure calculations were supported by the state assignment of Minobrnauki of Russia (theme "Electron" No. AAAA-A18-118020190098-5).

- 
- [1] J. G. Bednorz and K. A. Müller, Possible high  $T_c$  superconductivity in the Ba-La-Cu-O system, *Zeitschrift für Physik B Condensed Matter* **64**, 189 (1986).
- [2] C. C. Tsuei and J. R. Kirtley, Pairing symmetry in cuprate superconductors, *Rev. Mod. Phys.* **72**, 969 (2000).
- [3] D. J. Scalapino, A common thread: The pairing interaction for unconventional superconductors, *Rev. Mod. Phys.* **84**, 1383 (2012).
- [4] P. A. Lee, N. Nagaosa, and X.-G. Wen, Doping a Mott insulator: Physics of high-temperature superconductivity, *Rev. Mod. Phys.* **78**, 17 (2006).
- [5] J. Zaanen, G. A. Sawatzky, and J. W. Allen, Band gaps and electronic structure of transition-metal compounds, *Phys. Rev. Lett.* **55**, 418 (1985).
- [6] F. C. Zhang and T. M. Rice, Effective Hamiltonian for the superconducting Cu oxides, *Phys. Rev. B* **37**, 3759(R) (1988).
- [7] E. Pavarini, I. Dasgupta, T. Saha-Dasgupta, O. Jepsen, and O. K. Andersen, Band-Structure Trend in Hole-Doped Cuprates and Correlation with  $T_{cmax}$ , *Phys. Rev. Lett.* **87**, 047003 (2001).
- [8] H. Sakakibara, H. Usui, K. Kuroki, R. Arita, and H. Aoki, Two-Orbital Model Explains the Higher Transition Temperature of the Single-Layer Hg-Cuprate Superconductor Compared to That of the La-Cuprate Superconductor, *Phys. Rev. Lett.* **105**, 057003 (2010).
- [9] J. Choisnet, R.A. Evarestov, I.I. Tupitsyn and V.A. Veryazov, Investigation of the chemical bonding in Nickel mixed oxides from electronic structure calculations, *J. Phys. Chem. Solids* **157**, 1839 (1996).
- [10] M.J. Martínez-Lope, M.T. Casais, J.A. Alonso, Stabilization of  $\text{Ni}^{1+}$  in defect perovskites  $\text{La}(\text{Ni}_{1-x}\text{Al}_x)\text{O}_{2+x}$  with 'infinite-layer' structure, *J. Alloys and Compounds* **275**, 109 (1998).
- [11] M. A. Hayward, M. A. Green, M. J. Rosseinsky, and J. Sloan, Sodium Hydride as a Powerful Reducing Agent for Topotactic Oxide Deintercalation: Synthesis and Characterization of the Nickel(I) Oxide  $\text{LaNiO}_2$ , *J. Am. Chem. Soc.* **121**, 8843 (1999).
- [12] A. Ikeda, T. Manabe, M. Naito, Improved conductivity of infinite-layer  $\text{LaNiO}_2$  thin films by metal organic decomposition, *Physica C* **495**, 134 (2013).
- [13] K.-W. Lee and W.E. Pickett, Infinite-layer  $\text{LaNiO}_2$ :  $\text{Ni}^{1+}$  is not  $\text{Cu}^{2+}$ , *Phys. Rev. B* **70**, 165109 (2004).
- [14] V. I. Anisimov, D. Bukhvalov, and T. M. Rice, Electronic structure of possible nickelate analogs to the cuprates, *Phys. Rev. B* **59**, 7901 (1999).
- [15] D. Li *et al.*, Superconductivity in an infinite-layer nickelate, *Nature* **572**, 624 (2019).
- [16] D. Li, B. Y. Wang, K. Lee, S. P. Harvey, M. Osada, B. H. Goodge, L. F. Kourkoutis, H. Y. Hwang, Superconducting Dome in  $\text{Nd}_{1-x}\text{Sr}_x\text{NiO}_2$  Infinite Layer Films, *Phys. Rev. Lett.* **125**, 027001 (2020).
- [17] S. Zeng *et al.*, Phase diagram and superconducting dome of infinite-layer  $\text{Nd}_{1-x}\text{Sr}_x\text{NiO}_2$  thin films, arXiv:2004.11281 (2020).
- [18] M. Osada, B. Y. Wang, B. H. Goodge, K. Lee, H. Yoon, K. Sakuma, D. Li, M. Miura, L. F. Kourkoutis, H. Y. Hwang, A superconducting praseodymium nickelate with infinite layer structure, arXiv:2006.13369 (2020).
- [19] M. Jiang, M. Berciu, and G. A. Sawatzky, *Phys. Rev. Lett.* **124**, 207004 (2020).
- [20] M.-Y. Choi, K.-W. Lee and W.E. Pickett, Role of 4f states in infinite-layer  $\text{NdNiO}_2$ , *Phys. Rev. B* **101**, 020503(R) (2020).
- [21] V. Olevano, F. Bernardini, X. Blase, and A. Cano, Ab initio many-body GW correlations in the electronic structure of  $\text{LaNiO}_2$ , *Phys. Rev. B* **101**, 161102(R) (2020).
- [22] Y. Nomura, M. Hirayama, T. Tadano, Y. Yoshimoto, K. Nakamura, and R. Arita, Formation of a two-dimensional single-component correlated electron system and band engineering in the nickelate superconductor  $\text{NdNiO}_2$ , *Phys. Rev. B* **100**, (2019).
- [23] Z. Liu, Z. Ren, W. Zhu, Z. Wang and J. Yang, Electronic and magnetic structure of infinite-layer  $\text{NdNiO}_2$ : trace of antiferromagnetic metal, *npj Quantum Materials* **5**:31 (2020).
- [24] J. Gao, Z. Wang, C. Fang, H. Weng, Electronic structures and topological properties in nickelates  $\text{Ln}_{n+1}\text{Ni}_n\text{O}_{2n+2}$ , arXiv:1909.04657 (2019).
- [25] J. Karp, A. S. Botana, M. R. Norman, H. Park, M. Zingl and A. Millis, Many-body Electronic Structure of  $\text{NdNiO}_2$  and  $\text{CaCuO}_2$ , *Phys. Rev. X* **10**, 021061 (2020).
- [26] M. Hepting *et al.*, Electronic structure of the parent compound of superconducting infinite-layer nickelates, *Nature*

- ture Materials **19**, 381 (2020).
- [27] Y. Gu, S. Zhu, X. Wang, J. Hu and H. Chen, A substantial hybridization between correlated Ni-d orbital and itinerant electrons in infinite-layer nickelates, *Communications Physics* **3**, 84 (2020).
- [28] A.S. Botana and M.R. Norman, Similarities and Differences between  $\text{LaNiO}_2$  and  $\text{CaCuO}_2$  and Implications for Superconductivity, *Phys. Rev. X* **10**, 011024 (2020).
- [29] X. Wu, D. D. Sante, T. Schwemmer, W. Hanke, H. Y. Hwang, S. Raghu, and R. Thomale, Robust  $d_{x^2-y^2}$ -wave superconductivity of infinite-layer nickelates, *Phys. Rev. B* **101**, 060504(R) (2020).
- [30] E. Been, W.-S. Lee, H. Y. Hwang, Y. Cui, J. Zaanen, T. Devereaux, B. Moritz, C. Jia, Theory of Rare-earth Infinite Layer Nickelates, arXiv:2002.12300 (2020).
- [31] H. Zhang, L. Jin, S. Wang, B. Xi, X. Shi, F. Ye, and J.-W. Mei, Effective Hamiltonian for nickelate oxides  $\text{Nd}_{1-x}\text{Sr}_x\text{NiO}_2$ , *Phys. Rev. Research* **2**, 013214 (2020).
- [32] S. Ryee, H. Yoon, T. J. Kim, M. Y. Jeong, and M. J. Han, Induced magnetic two-dimensionality by hole doping in the superconducting infinite-layer nickelate  $\text{Nd}_{1-x}\text{Sr}_x\text{NiO}_2$ , *Phys. Rev. B* **101**, 064513 (2020).
- [33] Y. Nomura, T. Nomoto, M. Hirayama, R. Arita, Magnetic exchange coupling in cuprate-analog  $d^9$  nickelates, arXiv:2006.16943 (2020).
- [34] M.-Y. Choi, W. E. Pickett and K.-W. Lee, Quantum-Fluctuation-Frustrated Flat Band Instabilities in  $\text{NdNiO}_2$ , arXiv:2005.03234 (2020).
- [35] L. Si, W. Xiao, J. Kaufmann, J. M. Tomczak, Y. Lu, Z. Zhong, and K. Held, Topotactic Hydrogen in Nickelate Superconductors and Akin Infinite-Layer Oxides  $\text{ABO}_2$ , *Phys. Rev. Lett.* **124**, 166402 (2020).
- [36] C. Liu *et al.*, Observation of an antiferromagnetic quantum critical point in high-purity  $\text{LaNiO}_3$ , *Nature Commun.* **11**, 1402 (2020).
- [37] Y. Fu *et al.*, Core-level x-ray photoemission and Raman spectroscopy studies on electronic structures in Mott-Hubbard type nickelate oxide  $\text{NdNiO}_2$ , arXiv:1911.03177 (2020).
- [38] P. Jiang, L. Si, Z. Liao, and Z. Zhong, Electronic structure of rare-earth infinite-layer  $\text{RNiO}_2$  ( $R=\text{La}, \text{Nd}$ ), *Phys. Rev. B* **100**, 201106(R) (2019).
- [39] B. Geisler and R. Pentcheva, Fundamental difference in the electronic reconstruction of infinite-layer vs. perovskite neodymium nickelate films on  $\text{SrTiO}_3(001)$ , arXiv:2001.03762 (2020).
- [40] H. Sakakibara, H. Usui, K. Suzuki, T. Kotani, H. Aoki, K. Kuroki, Model construction and a possibility of cuprate-like pairing in a new  $d_9$  nickelate superconductor  $(\text{Nd}, \text{Sr})\text{NiO}_2$ , arXiv:1909.00060 (2019).
- [41] Byungkyun Kang, Corey Melnick, Patrick Semon, Gabriel Kotliar, Sangkook Choi, Infinite-layer nickelates as  $\text{Ni-e}_g$  Hund's metals, arXiv:2007.14610.
- [42] Z.-J. Lang, R. Jiang, W. Ku, Where do the doped hole carriers reside in the new superconducting nickelates?, arXiv:2005.00022 (2020).
- [43] F. Lechermann, Late transition metal oxides with infinite-layer structure: Nickelates versus cuprates, *Phys. Rev. B* **101**, 081110(R) (2020).
- [44] M. Kitatani, L. Si, O. Janson, R. Arita, Z. Zhong, K. Held, Nickelate superconductors – a renaissance of the one-band Hubbard model, arXiv:2002.12230 (2020).
- [45] F. Lechermann, Multiorbital processes rule the  $\text{Nd}_{1-x}\text{Sr}_x\text{NiO}_2$  normal state, arXiv:2005.01166 (2020).
- [46] I. Leonov, S. L. Skornyakov, and S. Y. Savrasov, Lifshitz transition and frustration of magnetic moments in infinite-layer  $\text{NdNiO}_2$  upon hole doping, *Phys. Rev. B* **101**, 241108(R) (2020).
- [47] L.H. Hu and C. Wu, Two-band model for magnetism and superconductivity in nickelates, *Phys. Rev. Research* **1**, 032046 (2019).
- [48] G.-M. Zhang, Y.-F. Yang, and F.-C. Zhang, Self-doped Mott insulator for parent compounds of nickelate superconductors, *Phys. Rev. B* **101**, 020501(R) (2020).
- [49] Y.-H. Zhang and A. Vishwanath, Type-II t-J model in superconducting nickelate  $\text{Nd}_{1-x}\text{Sr}_x\text{NiO}_2$ , *Phys. Rev. Research* **2**, 023112 (2020).
- [50] E. M. Nica, J. Krishna, R. Yu, Q. Si, A. S. Botana, O. Erten, Theoretical investigation of superconductivity in trilayer square-planar nickelates, arXiv:2003.09132 (2020).
- [51] P. Werner and S. Hoshino, Nickelate superconductors: Multiorbital nature and spin freezing, *Phys. Rev. B* **101**, 041104(R) (2020).
- [52] T. Zhou, Y. Gao, Z. D. Wang, Spin excitations in nickelate superconductors, *Sci. China-Phys. Mech. Astron.* **63**, 287412(2020).
- [53] X. Wan, Q. Yin, and S. Y. Savrasov, Calculation of Magnetic Exchange Interactions in Mott-Hubbard Systems, *Phys. Rev. Lett.* **97**, 266403 (2006).
- [54] A. I. Liechtenstein, M. I. Katsnelson, V. P. Antropov, and V. A. Gubanov, Local spin density functional approach to the theory of exchange interactions in ferromagnetic metals and alloys, *J. Magn. Magn. Mater.* **67**, 65 (1987).
- [55] X. Wan, J. Zhou, and J. Dong, The Electronic Structures and Magnetic Properties of Perovskite Ruthenates from Constrained Orbital-Hybridization Calculations, *Europhys. Lett.* **92**, 57007 (2010); Y. Du, H. Ding, L. Sheng, S. Y. Savrasov, X. Wan and C. Duan, Microscopic origin of stereochemically active lone pair formation from orbital selective external potential calculations, *J. Phys.: Condens. Matter* **26**, 025503 (2014).
- [56] S. Y. Savrasov, Linear-response theory and lattice dynamics: A muffin-tin-orbital approach, *Phys. Rev. B* **54**, 16470 (1996).
- [57] V. I. Anisimov, F. Aryasetiawan, and A. I. Liechtenstein, Firstprinciples calculations of the electronic structure and spectra of strongly correlated systems: The LDA+U method, *J. Phys. Condens. Matter* **9**, 767 (1997).
- [58] X. Wan, T. A. Maier, and S. Y. Savrasov, Calculated magnetic exchange interactions in high-temperature superconductors, *Phys. Rev. B* **79**, 155114 (2009).
- [59] Z.P. Yin, S. Lebegue, M.J. Han, B.P. Neal, S.Y. Savrasov and W.E. Pickett, Electron-hole symmetry and magnetic coupling in antiferromagnetic  $\text{LaFeAsO}$ , *Phys. Rev. Lett.* **101**, 047001 (2008); M.J. Han, Q. Yin, W.E. Pickett, S.Y. Savrasov, Anisotropy, Itineracy, and Magnetic Frustration in High-T-C Iron Pnictides, *Phys. Rev. Lett.* **102**, 107003 (2009).
- [60] X. Wan, J. Dong, and S. Y. Savrasov, Mechanism of magnetic exchange interactions in europium monochalcogenides, *Phys. Rev. B* **83**, 205201 (2011).
- [61] R. Nanguneri and S.Y. Savrasov, Exchange constants and spin waves of the orbital-ordered noncollinear spinel  $\text{MnV}_2\text{O}_4$ , *Phys. Rev. B* **86**, 085138 (2012).
- [62] D. Wang, X. Bo, F. Tang, and X. Wan, Calculated magnetic exchange interactions in the Dirac magnon material  $\text{Cu}_3\text{TeO}_6$ , *Phys. Rev. B* **99**, 035160 (2019).

- [63] G. Kotliar, S. Y. Savrasov, K. Haule, V. S. Oudovenko, O. Parcollet, C.A. Marianetti, Electronic Structure Calculations with Dynamical Mean-Field Theory, *Rev. Mod. Phys.* **78**, 865 (2006).
- [64] K. Haule, Quantum Monte Carlo impurity solver for cluster dynamical mean-field theory and electronic structure calculations with adjustable cluster base, *Phys. Rev. B* **75**, 155113 (2007).
- [65] F. Ronning, K. M. Shen, N. P. Armitage, A. Damascelli, D. H. Lu, Z.-X. Shen, L. L. Miller, and C. Kim, Anomalous high-energy dispersion in angle-resolved photoemission spectra from the insulating cuprate  $\text{Ca}_2\text{CuO}_2\text{Cl}_2$ , *Phys. Rev. B* **71**, 094518 (2005); D. S. Inosov, *et al.*, Momentum and Energy Dependence of the Anomalous High-Energy Dispersion in the Electronic Structure of High Temperature Superconductors, *Phys. Rev. Lett.* **99**, 237002 (2007).
- [66] Q. Yin, A. Gordienko, X. Wan, S. Y. Savrasov, Calculated Momentum Dependence of Zhang-Rice States in Transition Metal Oxides, *Phys. Rev. Lett.* **100**, 066406 (2008).
- [67] Y. Xiang, Q. Li, Y. Li, H. Yang, Y. Nie, H.-H. Wen, Magnetic transport properties of superconducting  $\text{Nd}_{1-x}\text{Sr}_x\text{NiO}_2$  thin films, arXiv:2007.04884 (2020).